E-Journal of Advanced Maintenance Vol.4 No.2 (2012) 96-104
Japan Society of Maintenology

Nondestructive Investigation of Wall Thinning in Doubled Layer Tube by Magnetic Adaptive Testing

Gábor VÉRTESY[1,†,*], Ivan TOMÁŠ[2], Tetsuya UCHIMOTO[1] and Toshiyuki TAKAGI[1]
[1] *Institute of Fluid Science, Tohoku University, 2-1-1 Katahira, Aoba-ku, Sendai 980-8577, Japan*
[2] *Institute of Physics, Na Slovance 2, Praha 182 2, Czech Republic*

(Received; For the use of JSM)

Abstract. A recently developed nondestructive method, called Magnetic Adaptive Testing, which is based on systematic measurement and evaluation of minor magnetic hysteresis loops was applied for detection of local wall thinning in carbon steel, ferromagnetic T-shape tubes. Presently no effective inspection method is available for detection of wall thinning of a T-tube with reinforcing plate. It was shown that an artificially made slot can be reliable detected with good signal/noise ratio from the other side of the specimen even through the support plate.

KEYWORDS: Magnetic NDT, Wall thinning, Magnetic Adaptive Testing

1. Introduction

For pipes used in industry, e.g. in chemical and power plants, wall thinning is one of the most serious defects [1, 2]. Detection and evaluation of the thickness reduction of pipes are very important issues for prediction of lifetime of the pipes in order to avoid severe accidents. Recently many nondestructive testing techniques, such as X-ray [3], microwave [4] ultrasonic [5-7], acoustic emission [8-10], eddy current [11], thermal infrared measurements [12] have been used for the measurement of pipe wall thinning. Currently the magnetic flux leakage (MFL) method is the most commonly used pipeline inspection technique [13-16].

Local wall thinning on the inner surface of a pipe (e.g. in a nuclear power plant) may occur due to the stream of coolant flowing inside the pipe, causing a serious problem of maintenance of the piping systems. The inspection should be done from the outer side of the pipe. In Japan there is a special concern on the local wall thinning at locations under an enforcement shield that covers outside of the pipe, where a branch pipe is connected to the main one. Because the enforcement shield and the pipe wall form two layers of metal, it is difficult to inspect inside of the pipe under the enforcement shield by ultrasonic thickness gauge. Pulsed eddy current testing technology was developed in recent years to detect wall thinning [17-19]. Because of its rich frequency components and applicability of large electric current, the pulsed eddy current method may show promising capability in detection and evaluation the defect in deep regions of the material. The feasibility of magnetic flux leakage method for estimation of wall thinning on pipes under reinforcing plates in nuclear power plants was also discussed. Assessment of size of a slit fabricated on underlayer of the layered specimen was shown to be possible from the flux leakage profile. Conditions of wall thinning under reinforcing plates can be monitored by MFL methods [20-21].

Another, recently developed nondestructive magnetic method (Magnetic Adaptive Testing, MAT) can also be successfully applied for the inspection of wall thinning in layered ferromagnetic materials [22,23]. MAT introduces a large number of magnetic descriptors to diverse variations in non-magnetic properties of ferromagnetic materials, from which those, optimally adapted to the just

[*]Corresponding author, E-mail: vertesy.gabor@ttk.mta.hu
[†] On leave from *Research Institute for Technical Physics and Materials Science, H-1121 Budapest, Konkoly Thege ut 29-33, Hungary*

ISSN – 1883 – 9894/09

investigated property and material, can be picked up. It was shown in [24] that Magnetic Adaptive Testing was an effective and promising tool for nondestructive detection of local thinning of a plate from the other side of the specimen. The method gave good results also in a layered ferromagnetic plates. It was proved by these model experiments, that a 9x2 mm^2 slot, made in a 3 mm thick ferromagnetic material could be well detected with good signal/noise ratio through one (or two) air-gap(s) and through 3-6 mm additional ferromagnetic material. The slot is seen not only in case when the measuring yoke is positioned exactly above it, but from about ±10 mm distance, too, with an acceptable signal/noise ratio.

The purpose of the present work is to apply MAT for detection of wall thinning in a big size, T shape, layered tube (used in nuclear power plants) made of ferromagnetic material.

2. Magnetic Adaptive Testing

Magnetic Adaptive Testing is based on systematic measurement and evaluation of minor magnetic hysteresis loops. For this purpose a specially designed Permeameter [25] with a magnetizing/sensing yoke is applied for measurement of families of minor loops of the magnetic circuit differential permeability. The block-scheme of the device and the sketch of the yoke can be seen in Fig. 1.

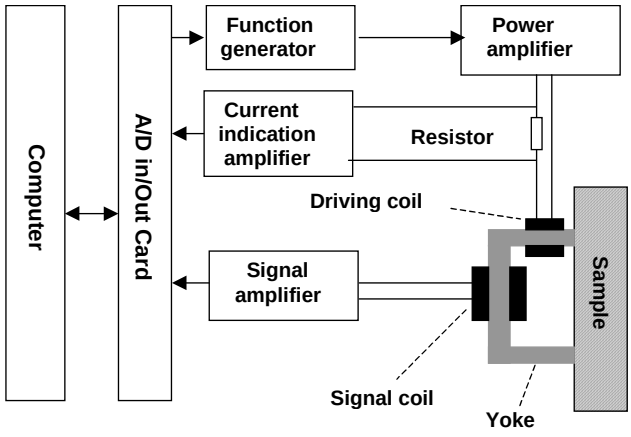

Fig. 1: Block-scheme of the Permeameter and sketch of the yoke.

The magnetizing coil wound on the yoke gets a triangular waveform current with step-wise increasing amplitudes and with a fixed slope magnitude in all the triangles. The voltage signal in the pick-up coil is proportional to the differential permeability of the magnetic circuit. The Permeameter works under full control of a PC computer, which sends the steering information to the function generator, and collects the measured data. An input-output data acquisition card accomplishes the measurement. The computer registers data-files for each measured family of the minor permeability loops. They contain detailed information about all the pre-selected parameters of the voltage signal induced in the pick-up coil. Before each measurement the sample is demagnetized by triangular waveform decreasing current. The raw data, which is registered for each sample characterized by a degradation parameter, ε_k, is a family of permeability loops, which is then processed by a special data-evaluation program. The program filters the experimental noise and interpolates the data into a regular square grid of elements, $\mu_{ij} \equiv \mu(F_i, A_j, \varepsilon_k)$, of a μ-matrix with a pre-selected magnetizing field step $\Delta F = \Delta A$. Here A_j is field amplitude of the j-th minor loop and F_i is current field value within that minor loop. The consecutive series of $\mu(\varepsilon_k)$-matrices, each taken for one sample with a value of the independent variable, ε_k, describes the magnetic reflection of the material degradation, ε. (ε can be any independent parameter, which characterize material modification, e.g. plastic deformation, fatigue, irradiation, thermal ageing, etc.) The matrices are processed by a matrix-evaluation program, which normalizes them by the matrix of a reference sample ($\varepsilon = \varepsilon_0$) chosen as the reference matrix, and arranges all the mutually corresponding elements $\mu_{ij}(\varepsilon_k)$ of all the evaluated $\mu(\varepsilon_k)$-matrices into a table.

Each $\mu_{ij}(\varepsilon)$-column of the table numerically represents dependence of one μ_{ij}-matrix element on the independent variable of the material degradation, ε. The dependence is referred to as the $\mu_{ij}(\varepsilon)$-degradation function. The most sensitive of all the degradation functions is found and it is then used for highly sensitive characterization of the investigated material.

Once the degradation functions are computed, the next task is to find the *optimum* degradation function(s) for the most sensitive and enough robust description of the investigated material degradation. A 3D-plot of sensitivity of the degradation functions can substantially help to choose the optimum one(s). The matrix-evaluation program calculates also sensitivity of each degradation function and draws their "sensitivity map" in the plane of the field coordinates $(F_i,A_j)\equiv(i,j)$. A 3D-plot of sensitivity of the degradation functions can substantially help to choose the optimum one(s). This map shows relative sensitivity of each $\mu_{ij}(\varepsilon)$-degradation function with respect to the independent variable, ε, of the investigated material. Sensitivity of each degradation function is computed as the slope of its linear regression and it is expressed by a color and/or shade in the sensitivity map figure. The sensitivity map gives useful information about the relative change of the investigated magnetic descriptor with respect to the independent variable (the top of the "hills" are those area(s) from where the most sensitive MAT-degradation functions can be taken). On the other side it also indicates, how reliably the parameter can be determined if the measurement is repeated (large plateaus are favorable from this point of view, where parameters depend only very slightly from the actual choice of the exact field coordinates values F_i and A_i).

By integration and/or differentiation of permeability along the field, F_i, *B*-matrices and/or μ'-matrices can be obtained. The *B*- and μ'-matrices contain in principle the same information as the μ-matrices, however, the corresponding $B(\varepsilon)$- and $\mu'(\varepsilon)$-degradation functions are different and sometimes more advantageous.

The paragraphs above describe the method of MAT as it is used for determination of the most sensitive characterization (i.e. of the most sensitive degradation function) of variation of the material properties of different samples, typically referred to as the "*material degradation*". In the case of the investigation of *local thinning of a tube* of ferromagnetic material, the sample should be *scanned* by the magnetizing/sensing yoke in a sequence of pre-determined positions, x_k, of the yoke on the surface of the tube. Measurement at each position, x_k, is then characterized by one $\mu(x_k)$-matrix, and similarly as in the above paragraph $\mu_{ij}(x)$-degradation functions are constructed. Then, the most sensitive of all the $\mu_{ij}(x)$-degradation functions is found and used for highly sensitive determination of the yoke position x_D, under which the thinning of the tube (i.e. the defect) is situated. Most suitably, the position of the yoke x_0, under which there is no defect, and which is far from the specimen boarders, is used for normalization.

The measuring conditions form an open magnetic circuit, where the exact value of magnetizing fields is difficult to express. Because of this, magnitudes of the magnetizing field, F_i, and of the minor loop amplitude, A_i, will be characterized by corresponding values of the applied magnetizing currents, given in Amps, in all the following text.

3. Influence of the sample thickness on the measured MAT signal

In order to show background of the technique, preliminary measurements were performed on a system of carbon steel plates, demonstrating influence of the sample thickness on the measured MAT signal. It was studied, as presented in [24], what modifications of the measured signal can be expected if the compared samples have different thickness.

(a) Generally it can be expected that thick or large samples, if magnetized by a single yoke attached from one side, are magnetized less uniformly than thin or small samples. As a consequence of this, the induced signal can be expected more "blurred" ("lower and wider") on thick and large samples than on thin and small ones, where it can be expected sharp and narrow. Signal on samples of large dimensions can be understood as integrated from all the large body of the sample, where the magnetic conditions are not very uniform.

(b) However, also generally, it can be probably expected, that signal of thick and large samples will be larger than signal measured by the same magnetizing head on thin and small samples. The reason for this statement is that the cross-section of the thick and large samples is larger, i.e. their

magnetic resistance is smaller. Evidently, the tendencies (a) and (b) do not work exactly in the same direction, actually they can work to some extent against each other and some work on optimization of the yoke dimensions with respect to different samples will be needed.

For checking validity of the above considerations and to see the influence of sample thickness on the measured signal, two flat samples with different thicknesses (3 and 6 mm) and the same lateral dimensions (100 mm x 100 mm) were measured by MAT. The samples were prepared from commercial low carbon steel (CSN 12050) material. Each sample is one piece of a "continuous" steel. The samples were measured by attaching a magnetizing yoke on the surface of the sample. The yoke was a C-shaped laminated Fe-Si transformer core. Fig. 2 shows comparison of the two samples, where the primarily measured MAT signal is shown for the two differently thick plates. As clearly seen, the signal of thicker samples is wider and larger than signal of the thinner samples. Both (a) and (b) rules hold. These preliminary experiments verified that different signal – and different MAT degradation functions – are expected if the thickness of the measured plate sample is locally modified. These considerations mean the theoretical background of wall thinning measurements.

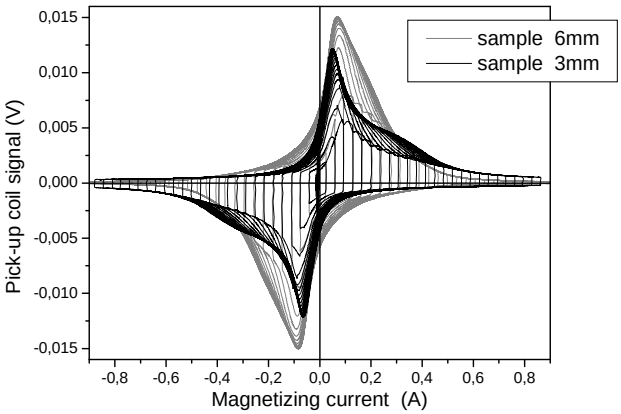

Fig. 2. Sample thickness effect on MAT signal, measured on two flat plates with different, 3 and 6 mm thicknesses [24].

4. Experimental

Experiments were performed on a layered T-shape carbon steel tube (outer layer is the reinforcing plate) which simulates the T-tubes in nuclear power plants. It contained an artificial slot. The main tube is STB410 500A sch60 (JIS) whose diameter is 508 mm. The branch tube installed to the main tube perpendicularly is STB410 400A sch60 (JIS) and its diameter is 406 mm. Circular cover plate made of SB410 (JIS) with the diameter of 400 mm were forged and welded to the main and branch tubes. The wall of the main tube is 20 mm thick, and the cover plate is 10 mm thick. The photograph of the tube is given in Fig. 3. The magnetizing yoke, used for magnetic measurement, can also be seen in the picture. (The arrow indicates the direction of the scanning of the yoke. See also Fig. 4.) An artifial slot was fabricated in the inner side of the main tube (not seen on the picture, but it is located moreorless under the magnetizing yoke). Its area is 50x20 mm^2, and it is 10 mm deep.

The measurement was performed on the tube of Fig. 3, as shown in Fig. 4. The magnetizing yoke was placed outside, as it is seen in Fig. 3. The yoke was a C-shaped laminated Fe-Si transformer core. The total outside length of the yoke is 105 mm (perpendicular to *x* direction), the legs of the yoke are 40x30 mm^2, the gap between legs is 45 mm. A magnetizing coil (N=105) and a pick-up coil (N=35) are wound on the legs of the core. The yoke was moved step by step along the tube's surface, perpendicular to the axis of the large tube, as indicated in Figs. 3 and 4 by the arrow, and measurements were performed at each position. The sketch of the tube and the measurement arrangement is shown in Fig. 4. The distance from the yoke to the branch tube was 23 mm, and the distance from the yoke to the plate edge was 44 mm. The presence of the slot was determined by scanning the yoke along the „Measurement" line. A reference measurement was also performed along the „Reference measurement" line.

Fig. 3. Photograph of the T-shape tube with the magnetizing yoke placed on the top tube. The arrow shows the direction of movement of the magnetizing yoke (x direction).

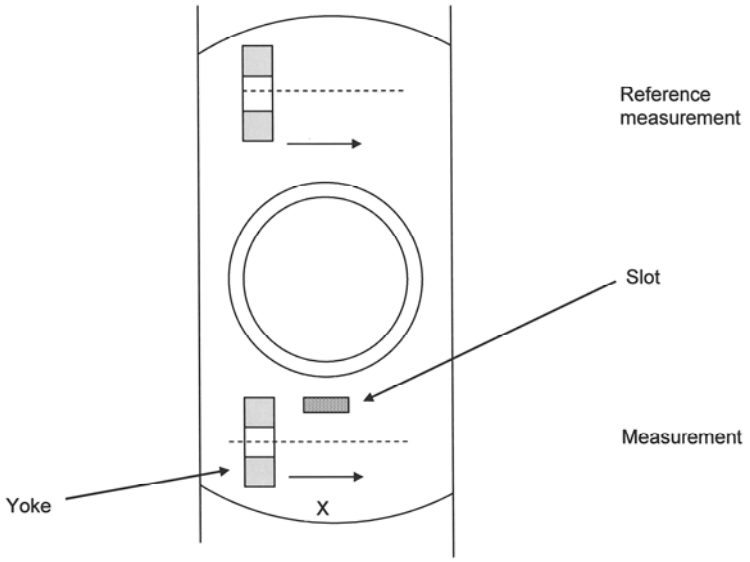

Fig. 4. The sketch of the tube and the measurement. Dashed lines show how the center of the yoke moves during the measurement (along *x* direction).

5. Results and discussion

As described above, the measurement was performed by positioning of the yoke along the *x* line. The signals of the pick up-coil for three different positions of the yoke are shown in Fig. 5. x = -60 mm means the position of the yoke, farest from the slot, while at x = 0 mm the center of yoke was above the center of the slot. The magnetic contact between the tube's surface and magnetizing yoke was not good, because the leg of the yoke was flat, which touched the surface of the tube only along a line. Nevertheless, the measured permeability loops were acceptable, the sample was magnetized relatively well, as it is reflected on the measured permeability plots, shown in Fig. 5. For future

applications, curved surface of the yoke's leg (according to the radius of the tube) should be prepared, which probably will result better quality magnetic contact and perhaps even better results.

The modification of the shape of permeability loops, due to the existence of the slot under the magnetizing yoke is seen very well, and it is in good correlation with the phenomenon, observed on samples having different thickness (see Fig. 2). Theory works well.

MAT degradation functions were evaluated as functions of the yoke position. The center of the slot is at x = 0 mm. Each MAT degradation function is normalized by the corresponding one, which belongs to the x = -60 mm position (farest from the slot). The best degradation functions were obtained if the reciprocal values of $\mu'(x)$-degradation functions were considered. "Best" means that largest sensitivity and best reproducibility can be achieved in the case of these degradation functions. The optimally chosen degradation functions are shown in Fig. 6, while the correspondig sensitivity map is given in Fig. 7. This map does not give directly the values of $1/\mu_{ij}'(x)$-degradation function, but shows the relative sensitivity of each $1/\mu_{ij}'(x)$-degradation function with respect to the position of the yoke, x. Sensitivity of each degradation function is computed as the slope of its linear regression and it is expressed by a color and/or shade in the sensitivity map figure. Red areas corresponds to the top sensitivity values. It gives (F_i,A_j) pairs, and in the knowledge of these values most sensitive $1/\mu_{ij}'(x)$ values can be determined. In our case optimal MAT degradation function can be taken from two areas of the sensitivity map, which are identical with each other from this point of view. These areas appear with red color in Fig. 7, and represents those degradation functions, which exhibit the largest sensitivity of the modification of MAT parameters while the yoke is moving along the measurement line. The crosses of lines in the sensitivity map of the $1/\mu'$-degradation functions show the centers of the areas, from where the points of Fig. 6 are taken (F_i=90mA, A_i=240mA) and (F_i=240mA, A_i=300mA). It is important to mention that the areas of these top sensitivity degradation functions are rather large, and the "hill" is smooth enough, which ensures good reproducibility and reliability of the chosen MAT descriptors. (The area between F=0 and F=75 mA is not suitable for choosing reliable MAT parameters, in spite of the large sensitivity, because in this area the reproducibility of parameters is poor due to the large scatter of points.)

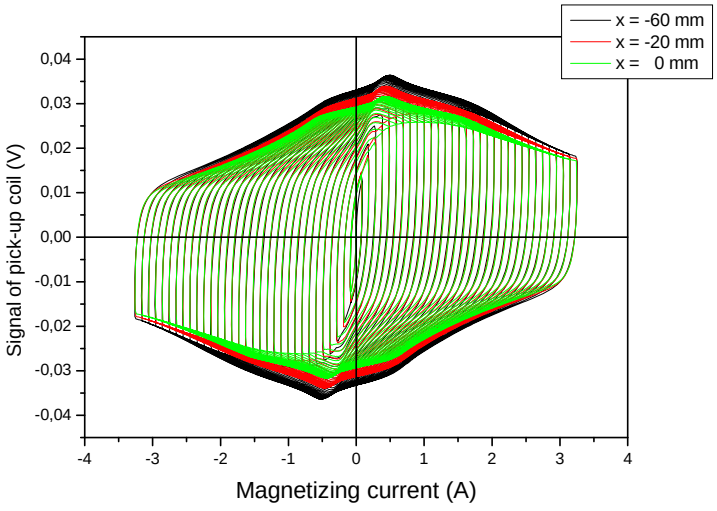

Fig. 5. Examples of families of the μ-shaped loops vs. magnetizing current measured at three different positions of the magnetizing yoke. The positive and negative parts of the signal correspond to the increasing and decreasing parts of the triangular waveform of the current (field), respectively.

It is demonstrated very well in the figure, that significant difference was found in MAT parameters between the reference position of the yoke and its position over the slot. The measurement was repeated several times with identical results, demonstrating reliability and reproducibility of this technique. About 40% difference is measured, which is caused by the local wall thinning. The largest values of the measured curve is over the center of the slot.

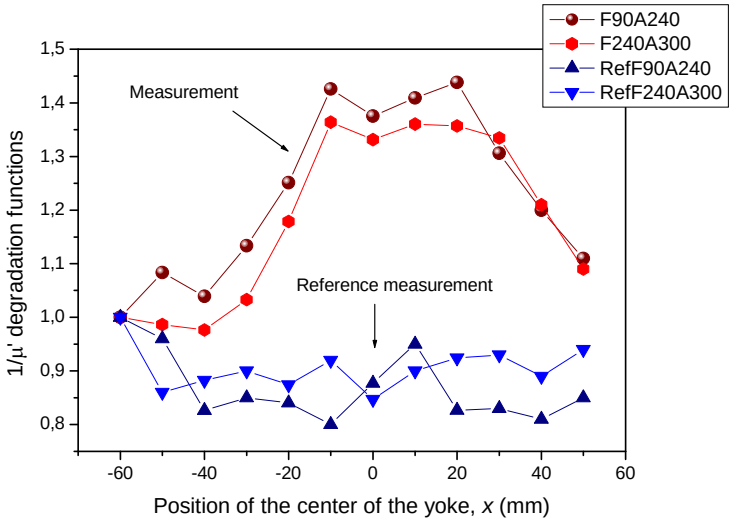

Fig. 6. The optimally chosen MAT degradation functions, taken from the two indicated areas of sensitivity map.

The fact, that a maximum is observed over the slot shows by itself that this is a real effect, not only an error of measurement. However, the complicated shape of the measured tube can influence the magnetic flux distribution inside the wall. In principle – as the worst case – it can happen that edge of the cover plate and/or existence of the perpendicular tube (which is rather close to the area of measurement) can perturb the measured permeability as a function of the yoke position. To be sure that really the existence of the inner slot was detected, the same measurement was also done on the other, symmetrical side of the perpendicular tube, where no artificial slot on the inner wall existed. This "reference measurement" line is shown in Fig. 4. For the reference evaluation the same (F_i,A_j) points, as in the case of "real" evaluation were used, as indicated in Fig. 6. In this case no difference of any MAT degradation function vs. the yoke position was detected, the measured point scatter over the normalized value. This was a direct and evident proof that the measurement really detected the slot.

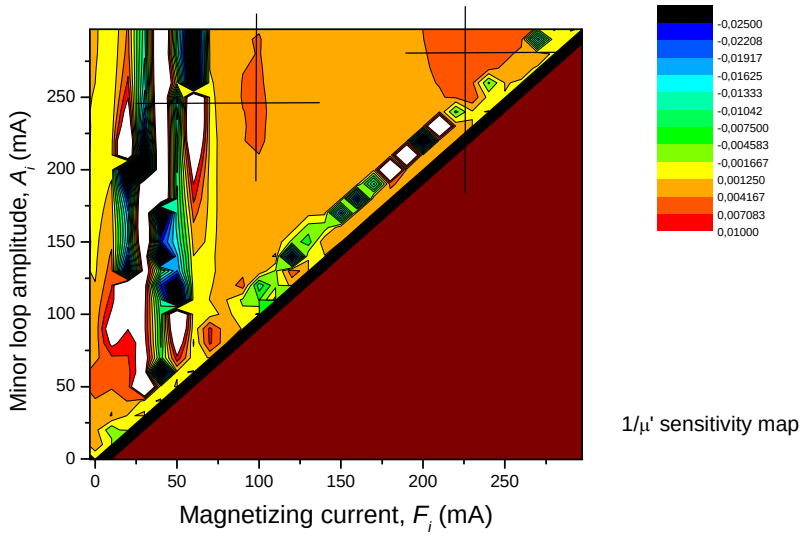

Fig. 7. Map of relative sensitivity of the $1/\mu'(x)$-degradation functions. The crossing point of the lines indicate field coordinates of the most sensitive $\mu_{ij}'(\varepsilon)$-degradation function, from where MAT degradation function of Fig. 6 were taken.

The determination of wall thinning by MAT measurements are affected by modifying the tube thickness and the size of magnetizing yoke. Many measurement series were performed previously on flat samples to find the optimal relation between the thickness of the sample and the size of the yoke. The above described experiment was performed in a given tube, with given tube thickness. The size of magnetizing yoke was chosen according to this tube thickness This size is believed to be close to the optimal one.

By applying this type of magnetic measurements, the results are also affected both by the surface conditions of the tube and also by the clearance between the top plate and the main tube. Results are influenced by existence of the uncontrolled little air gap between the applied yokes and the samples. Quality of magnetic contact between the sample surface and faces of the yoke has a strong influence on the measured signal and especially with unpolished surfaces it is difficult to be reproduced. However, if the conditions are similar in all the tested cases (there are no big differences of surface roughness from measurement to measurement) the measurements can be performed with good reproducibility and reliability. This is the case in the presently shown experimens. For future measurements, where the surface conditions are not rigorously kept constant, the scatter of points can be reduced significantly by applying a nonmagnetic spacer between the sample surface and yoke. It has been demonstrated recently [26], that spacers placed between the sample surface and faces of the yokes decreased fluctuation of quality of the magnetic contact from sample to sample. The spacers smoothed down scatter of the measured signal values, the measurement became more reliable, but sensitivity of the μ-degradation functions was decreased at the same time. However, presence of the spacers also modified shapes of the signals and their derivatives. As a result μ'-degradation functions computed from the first derivative of the signal with an optimally chosen spacer acquired extreme sensitivity, while keeping still very satisfactory scatter of the measured points.

The influence of the clearance between the tubes was not investigated in the present case, because the tube system was given. However, many measurements were also performed to study this phnomenon, and it was found that up to a certain size of clearance between ferromagnetic plates MAT can be successfully applied.

6. Conclusions

The above outlined result illustrates that Magnetic Adaptive Testing is a suitable technique for inspection of wall thinning in thick, layered carbon steel tubes. The existence of an artifical slot could be detected with good signal/noise ratio and with good reliability even under an enforcement shield that covers outside of the pipe. Further experiments are needed to optimize the size and shape of the magnetizing yoke, and to determine the smallest detectable size of the thinned area of the wall.

Acknowledgements

This study was performed as a part of "Project on enhancement of aging management and maintenance of NPPs" supported by nuclear and industrial safety agency, METI, JAPAN. The work was also supported by Hungarian Scientific Research Fund (project A08 CK 80173), by project No.101/09/1323 of the Grant Agency of the Czech Republic and by the Hungarian-Czech Bilateral Intergovernmental S&T Cooperation project.

References

[1] H.M. Crockett, J.S. Horowitz, J. Pressure Vessel Technology, 132 (2010) 024501-1
[2] I. Nishiguchi, F. Inada, M. Takahashi, B. Ogawa, T. Inagaki, T. Ohira, K. Iwahara, K. Yamakami, E-Journal of Advanced Maintenance, 2 (2010/2011) 14-24.
[3] G. Kajiwara, J. of Testing and Evaluation, 33 (2005) 574-583
[4] Yang Ju, Advanced Nondestructive Evaluation II, Volume 2 (2007) 1128-1133
[5] K.R. Leonard, M.K. Hinders, Ultrasonic, 43 (2005) 574-583
[6] Z. Cho, W.D. Oh, J.H. Lee, Key Engineering Materials, 321-323 (2006) 795-798
[7] D.H Lee, S.J Lee, J.H Lee, S.H. Lee, AIP Conf. Proc., Vol. 975, (2008) 1732-1738
[8] K.W. Nam, S.H. Ahn, Key Engineering Materials, 270-273 (2004) 461-465
[9] K. Mitani, M. Mochizuki, M. Toyoda, Materials Science Forum, 580 – 582 (2008) 113-116
[10] D. Kosaka, F. Kojima, H. Yamaguchi, International Journal of Applied Electromagnetics and Mechanics, 33 (2010)
[11] T. R. Schmidt, Materials Evaluation, vol. 42 (1984) 225-230
[12] A.I.N. Linkous, B. McKnight, Proc. SPIE Vol. 1933, p. 26-30, Thermosense XV: An International Conference on Thermal Sensing and Imaging Diagnostic Applications, Lee R. Allen; Ed.
[13] H. Zuoying, Q. Peiwen, C. Liang, NDT & E International, 39 (2006) 61-66
[14] A. Joshi, L. Udpa, S. Udpa, A. Tamburrino, IEEE Transactions on Magnetics, 42 (2006) 3168-3170
[15] Xiang Li, Xunbo Li, Liang Chen, Guangxu Qin, Peifu Feng, Zuoying Huang, IEEE International Conference on Industrial Technology (IEEE ICIT 2008), pp. 1-4
[16] H. Kikuchi, Y. Kurisawa, K. Ara, et al., Int. J. Appl. Electromagnetics and Mechanics, 33 (2010) 1087-1094
[17] C.S. Angani, D.G. Park, G.D. Kim, C.G. Kim, Y.M. Cheong, Journal of Applied Physics 107 (2010) pp. 09E720 - 09E720-3
[18] J. Kim, G. Yang, L. Udpa, S. Udpa, NDT & E International, 43 (2010) 141-144
[19] S. Xie, T. Yamamoto, T. Takagi, T. Uchimoto, in Electromagnetic Nondestructive Evaluation (XIV), Eds: T. Chady et al, IOS Press, 2011, pp. 203-210
[20] H. Kikuchi, K. Sato, I. Shimizu, Y. Kamada, S. Kobayashi, IEEE Trans. Magn. 47 (2010) 3963-3966
[21] H. Kikuchi, I. Shimuzu, K. Ara, Y. Kamada, S. Kobayashi, in Electromagnetic Nondestructive Evaluation (XIV), Eds: T. Chady et al, IOS Press, 2011, pp. 275-281
[22] I. Tomáš, J. Magn. Magn. Mat. 268 (2004) 178
[23] I. Tomáš, G. Vértesy, „Magnetic Adaptive Testing“, chapter in book „Nondestructive Testing“ (Editor M.Omar), InTech-d.o.o. - Open Access publisher: www.intechopen.com, (ISBN 979-953-307-487-9), 2012
[24] G. Vértesy, I. Tomáš T. Uchimoto, T. Takagi, NDT & E International, 47 (2012) 51-55
[25] I. Tomáš, O. Stupakov, J. Kadlecová, O. Perevertov, J. Magn. Magn. Mat., 304 (2006) 168-171
[26] I. Tomáš, J. Kadlecová, G. Vértesy, IEEE Trans Magn, 48 (2012) 1441